

Symmetry-Breaking Lattice Distortion in $\text{Sr}_3\text{Ru}_2\text{O}_7$

C. Stingl,¹ R. S. Perry,^{2,3,4} Y. Maeno,^{3,4} and P. Gegenwart¹

¹*I. Physikalisches Institut, Georg-August-Universität Göttingen, D-37077 Göttingen, Germany*

²*Scottish Universities Physics Alliance, School of Physics, University of Edinburgh, Mayfield Road, Edinburgh EH9 3JZ, Scotland*

³*International Innovation Center, Kyoto University, Kyoto 606-8501, Japan*

⁴*Department of Physics, Kyoto University, Kyoto 606-8502, Japan*

(Received 21 December 2010; published 6 July 2011)

The electronic nematic phase of $\text{Sr}_3\text{Ru}_2\text{O}_7$ is investigated by high-resolution in-plane thermal expansion measurements in magnetic fields close to 8 T applied at various angles Θ off the c axis. At $\Theta < 10^\circ$ we observe a very small (10^{-7}) lattice distortion which breaks the fourfold in-plane symmetry, resulting in nematic domains with interchanged a and b axis. At $\Theta \geq 10^\circ$ the domains are almost fully aligned and thermal expansion indicates an area-preserving lattice distortion of order 2×10^{-6} which is likely related to orbital ordering. Since the system is located in the immediate vicinity of a metamagnetic quantum critical end point, the results represent the first observation of a structural relaxation driven by quantum criticality.

DOI: [10.1103/PhysRevLett.107.026404](https://doi.org/10.1103/PhysRevLett.107.026404)

PACS numbers: 71.10.Hf, 71.27.+a, 75.30.Kz

Electronic nematic states in condensed matter have been recently considered quantum analogues of nematic liquid crystals which display directional but no positional order [1]. Their ground state is intermediate between insulating “crystals” and isotropic metallic (Fermi) liquids. Upon forming an electronic nematic phase, the point-group symmetry of the underlying host crystal is spontaneously broken, resulting in anisotropic electronic properties which could most easily be detected by charge or heat transport measurements along different crystallographic directions [2]. A spontaneous generation of spatial anisotropy has been found in quantum Hall systems, cuprate and iron-pnictide high-temperature superconductors as well as in the bilayer ruthenate $\text{Sr}_3\text{Ru}_2\text{O}_7$ [3–6]. In the case of the cuprates, the nematicity characterizes the yet unidentified pseudogap state while for iron pnictides it precedes the orthorhombic lattice distortion and spin-density-wave formation. However, as the fourfold rotational symmetry in these cases is already broken by the lattice, the transport anisotropy arising from electronic nematicity needs to be carefully distinguished from the one resulting from the crystal lattice alone [2]. In this respect, $\text{Sr}_3\text{Ru}_2\text{O}_7$ is considered as a cleaner example as its nematic order develops out of a fourfold symmetric state and is not accompanied by magnetic ordering or charge-density-wave formation. In this Letter, we prove by high-resolution dilatometry that the nematicity in $\text{Sr}_3\text{Ru}_2\text{O}_7$ is related to a spontaneous symmetry-breaking lattice distortion, representing the first example of a structural relaxation driven by strong electronic correlations near a quantum phase transition.

The bilayer perovskite ruthenate $\text{Sr}_3\text{Ru}_2\text{O}_7$ has initially attracted considerable attention due to a field-induced quantum critical point (QCP) near 8 T ($B \parallel c$), which is associated with itinerant-electron metamagnetism [7]. Subsequent studies on ultrahigh-quality samples revealed

thermodynamic evidence for the formation of a novel phase below 1 K, bounded in field by two first-order metamagnetic transitions, which intervenes in the approach of the QCP [8]. Within this phase, the electrical resistivity reaches a maximum and becomes temperature independent, indicating a reduction of the charge carrier mean free path. This has been ascribed to the formation of domains resulting from a Pomeranchuk-like Fermi surface distortion. As the magnetic field is tilted by a small angle of $\Theta = 13^\circ$ towards the ab plane, the in-plane resistivity develops a pronounced anisotropy within the phase, suggesting the formation of an electronic nematic fluid [6]. The isotropic resistivity behavior at $B \parallel c$ would then arise from the random orientation of domains which could be aligned by an in-plane field.

The electronic structure of $\text{Sr}_3\text{Ru}_2\text{O}_7$ results from the partially filled Ru t_{2g} states hybridizing with the O p orbitals. The Fermi surface is complicated because of bilayer splitting of multiple bands, a 7° rotation of the RuO octahedra leading to a $\sqrt{2}$ reconstruction of the Brillouin zone, and spin-orbit coupling. Six bands have been experimentally identified [9], which have different quasi-one-dimensional (1D) (d_{yz} and d_{xz}) and quasi-two-dimensional (d_{xy}) orbital character. According to tight-binding band-structure calculations, the metamagnetic transitions and the nematic ordering result from the quasi-1D bands which are close to van Hove (vH) singularities [10–12]. The nematic state is characterized by a few percent difference in occupation between d_{yz} and d_{xz} derived bands. This (partial) “orbital ordering” breaks the fourfold rotational symmetry of the system. However, since electrons close to a vH singularity have a very small velocity, their influence on the charge transport in such a multiband system is negligible. Thus, the observed resistivity anisotropy must be related to domain wall scattering

rather than being intrinsic to the nematic phase [10]. If the domains are fully lined up, e.g., by an in-plane magnetic field, the resistivity should become insensitive to the nematic phase, although the nematic ordering could even be stronger. Therefore, dilatation measurements probing the intrinsic lattice anisotropy are a much better indicator for the nematic phase.

The measurements were performed on a high-quality single crystal studied previously by thermal expansion and magnetostriction along the c axis [8,13]. In order to determine the length change along the a axis while applying a field along the c axis, a miniaturized high-resolution capacitive dilatometer, which can be rotated in the bore of a superconducting magnet, has been utilized. Two parallel flat springs exert a uniaxial pressure of about 15 bar along the measurement direction $\parallel a$. The linear thermal expansion coefficient $\alpha(T)$ is obtained by calculating the slope of the relative length change in temperature intervals of 40 mK.

At first, we focus on the thermal expansion signature of the nematic phase for untilted magnetic fields ($B \parallel c$). As shown by the black line in Fig. 1(a), a distinct anomaly in the length change is found around 1 K which corresponds to a sharp discontinuity in the thermal expansion coefficient displayed in Fig. 1(b), indicative of a second-order phase transition, also found in specific heat measurements [14]. Note that our previous length measurements along the c axis have only detected a very small signature at the phase boundary [13], indicating that the nematic transition primarily affects the ab plane.

Next, we compare these data with corresponding measurements in a tilted magnetic field. In order to investigate the a axis length change parallel to the in-plane field, the entire dilatometer has been rotated in the bore of the superconducting magnet. In a second run to determine the

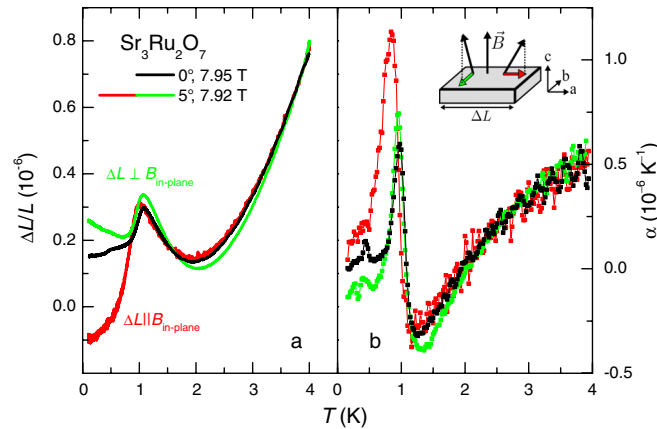


FIG. 1 (color online). In-plane relative length change $\Delta L/L$ (a) and respective thermal expansion coefficient $\alpha = d(\Delta L/L)/dT$ (b) vs temperature for $\text{Sr}_3\text{Ru}_2\text{O}_7$. The black curves represent data at a magnetic field of 7.95 T applied along the c axis, whereas the light gray (green) and gray (red) curves are taken at a field of 7.92 T tilted by 5° from the c axis with $\Delta L \perp B_{\text{in-plane}}$ and $\Delta L \parallel B_{\text{in-plane}}$, as sketched in the inset.

a -axis change perpendicular to the in-plane field, the sample has been rotated around a , while the dilatometer has been kept in its original position. In either case, the angle Θ with respect to the c axis has an error of $\pm 1^\circ$. As shown in Fig. 1, the tilting of the field has no significant effect at temperatures above 1.2 K. By contrast, a pronounced anisotropy evolves at the nematic transition, which is the central observation of this study. Despite the application of an in-plane field, the system retains its fourfold in-plane symmetry above the transition, which is then spontaneously broken at 1.2 K.

We have also studied the lattice anisotropy in the nematic phase at larger tilt angles, cf. Fig. 2. Compared to $\Theta \leq 5^\circ$, thermal expansion within the phase is much enhanced and the length changes parallel (ΔL_{\parallel}) and perpendicular (ΔL_{\perp}) to the in-plane field have similar size and opposite sign. This indicates an area-preserving lattice distortion of order 2×10^{-6} . This is still smaller than the instrumental resolution of elastic neutron scattering, which has failed to detect a splitting of the (020) peak [6]. Below 0.5 K Fermi liquid behavior $|\alpha| = a_1 T$ is found, with a highly enhanced coefficient $a_1 \approx 6 \times 10^{-6} \text{ K}^{-2}$, which is independent of B (within the nematic phase) and Θ (for $\Theta \geq 10^\circ$).

Our experiments strongly support the domain scenario described above. Since there is no difference in the observed distortion between the measurements at 10° and 15° , the sample appears to be effectively monodomain at $\Theta \geq 10^\circ$. The thermal expansion discontinuities at the nematic transition indicate that the a parameter of $\text{Sr}_3\text{Ru}_2\text{O}_7$ contracts (expands) along the direction parallel (perpendicular) to the in-plane field upon cooling through the nematic transition. Without an in-plane field, the

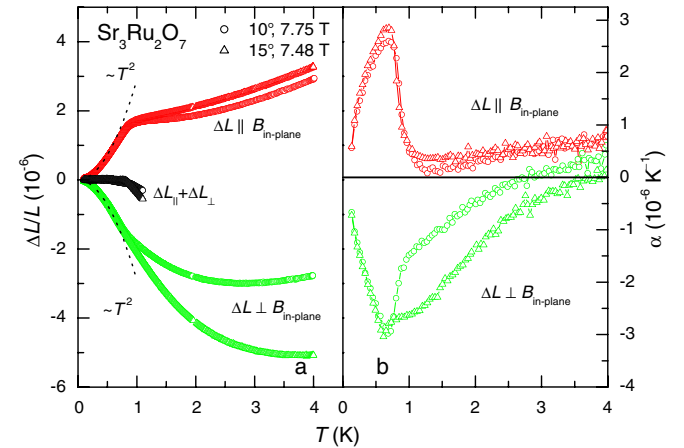


FIG. 2 (color online). In-plane relative length change (a) and thermal expansion (b) at magnetic fields of 7.75 T (circles) and 7.48 T (triangles) applied 10° and 15° off the c axis, respectively. For each angle, the length change has been determined parallel (gray or red symbols) and perpendicular (light gray or green symbols) to the in-plane component of the magnetic field. The dotted lines indicate T^2 behavior.

uniaxial pressure parallel to the measured a axis leads to a contraction upon cooling through the nematic transition (cf. Figure 1), although it is not sufficient to align all nematic domains. The contraction is enhanced by a superposed in-plane field along the direction of the uniaxial pressure while it is reduced for a perpendicular in-plane field.

We now turn to the measurements of the isothermal magnetostriction. At low temperatures, the nematic phase is bounded in field by two first-order metamagnetic transitions at $B_{c1} = 7.85$ T and $B_{c2} = 8.07$ T for $\Theta = 0$ [8]. Our previous c -axis dilatation measurements have detected two positive peaks in the magnetostriction coefficient in close similarity to respective peaks in the magnetic susceptibility, indicating a substantial magnetoelastic coupling, leading to an expansion of the c axis at each increase of the sample moment [8,15].

The lattice distortion in the nematic phase is most clearly reflected in low-temperature isothermal magnetostriction measurements along the a axis at angles $\Theta \geq 10^\circ$, cf. Fig. 3. Upon entering the phase at the lower metamagnetic transition, a pronounced expansion is found perpendicular to the in-plane field direction, whereas parallel to the in-plane field a contraction is observed. At B_{c2} the plane then mainly expands parallel to the in-plane field. This is compatible with an orthorhombic distortion as sketched in the inset.

Figure 4 displays the evolution of the phase diagram of $\text{Sr}_3\text{Ru}_2\text{O}_7$ with the tilt angle. At $\Theta = 0$, the nematic phase

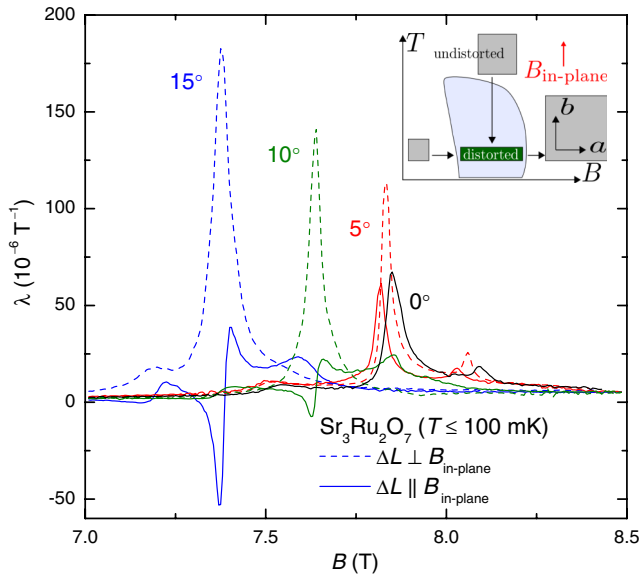


FIG. 3 (color online). Isothermal magnetostriction at temperatures below 0.1 K (cf. symbols in Fig. 4) of $\text{Sr}_3\text{Ru}_2\text{O}_7$ at different angles Θ of the applied field to the c axis. The solid and dotted curves represent data of the magnetostriction coefficient $\lambda = d(\Delta L/L)/dB$ along and perpendicular to the in-plane field, respectively. The inset shows a sketch of the lattice distortion in the nematic phase as derived from thermal expansion and magnetostriction measurements.

is bounded in field by two lines of first-order transitions ending at tricritical points [8] that are connected by a line of second-order phase transitions (indicated by the dash-dotted black line) [14]. An in-plane component of the magnetic field explicitly breaks the C_4 symmetry, leading to anisotropic behavior already outside the nematic phase. The nematic transition is then no longer defined by a spontaneous symmetry breaking. What was a nematic transition for $\Theta = 0$ should now be called metanematic transition in the presence of an in-plane field [17]. Specifically, the continuous transition above the critical points should become a crossover (cf. dotted lines), similar to the transition in an Ising ferromagnet in a small external symmetry-breaking field. The thermal expansion signature at the “roof” of the nematic phase changes with increasing Θ , but these data alone do not allow us to definitely classify the order of the transition.

The following scenario, sketched in Fig. 5, may account for our observations: The formation of the electronic nematic phase in $\text{Sr}_3\text{Ru}_2\text{O}_7$ leads to distorted domains with interchanged a and b axis, which can be aligned in tilted fields. These domains are responsible for the peak of the electrical resistivity [8]. The average domain wall separation is of the order of 500 nm [18]. Thermal expansion in tilted fields indicates that the domains are almost fully aligned for $\Theta \geq 10^\circ$. However, a few percent misaligned domains, which are hardly seen in thermal expansion, may still lead to additional scattering in the electrical resistivity. Most surprisingly, the resistivity peak is completely suppressed already at $\Theta \geq 5^\circ$ for the direction parallel to the

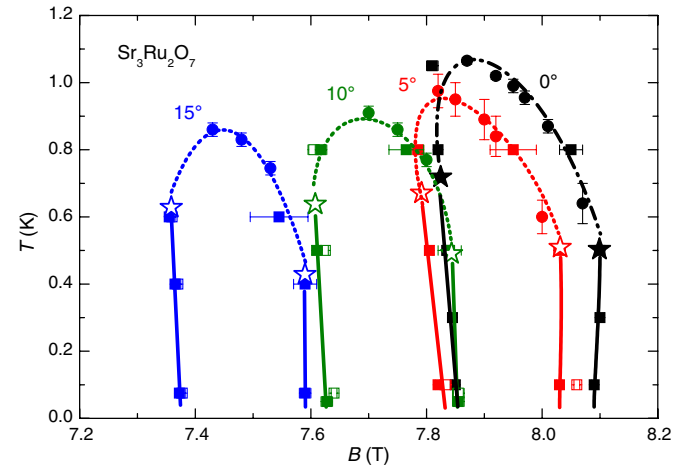


FIG. 4 (color online). Phase diagram of the nematic phase of $\text{Sr}_3\text{Ru}_2\text{O}_7$ at different tilt angles (cf. different colors). The squares and circles denote transitions in magnetostriction and thermal expansion, respectively (solid symbols: $\Delta L \parallel B_{\text{in-plane}}$, open symbols: $\Delta L \perp B_{\text{in-plane}}$). The black solid lines indicate first-order transitions ending at tricritical points (cf. filled stars) [8], connected by a (dash-dotted) line of second-order transitions. The colored open stars denote the presumed position of critical points, connected by crossover lines (dotted).

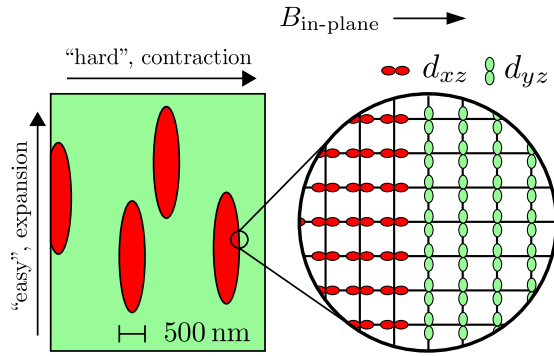


FIG. 5 (color online). Illustration of the proposed domain configuration (left, on macroscopic scale) and orbital ordering (right, on atomic scale) for the nematic phase of $\text{Sr}_3\text{Ru}_2\text{O}_7$ [12]. The different orbitally ordered states are indicated by the light gray (green) and gray (red) shading or color. The arrows indicate the directions of the in-plane field, easy and hard transport, as well as expansion and contraction.

in-plane field ("easy" transport direction), whereas it remains up to about 20° along the orthogonal direction ("hard" direction) [6]. This indicates that the domain wall scattering is highly anisotropic, likely because the domains are stretched along the easy transport direction. If an in-plane field along the in-plane x direction leads to a preferential occupation of the perpendicular d_{yz} orbitals [12], elongated domain walls perpendicular to the in-plane field are energetically favorable, since they do not break the d_{yz} orbital bonds. Consequently, a domain structure as sketched in Fig. 5 is stabilized. Our measurements prove that there is an expansion of the lattice along the easy transport direction parallel to the orbital bonds in the major domain. The Fermi surfaces responsible for the nematic ordering are holelike. Since electrons in holelike bands are similar to antibonding states in molecules, a reduction of the bandwidth due to a lattice expansion is favorable, as it reduces the kinetic energy of electrons in these states. Thus, the observed lattice distortion is consistent with the orbital ordering description of how fourfold rotational symmetry is broken in $\text{Sr}_3\text{Ru}_2\text{O}_7$ [19].

Finally, we comment on the general implications of our observations. Under certain conditions, fulfilled, e.g., for metamagnetic or valence instabilities, the order parameter fluctuations couple linearly to the lattice, leading to a divergence of the compressibility [20]. Then, the lattice may become unstable against a structural relaxation close to the QCP, as found in our experiments on $\text{Sr}_3\text{Ru}_2\text{O}_7$. This observation should motivate the search for other structural instabilities driven by quantum criticality and the development of models, taking into account the coupling between phonons and quantum critical fluctuations.

In conclusion, the electronic nematic phase in $\text{Sr}_3\text{Ru}_2\text{O}_7$ is characterized by an area-preserving symmetry-breaking lattice distortion of several 10^{-6} . If the symmetry is not broken explicitly by a sufficiently large in-plane field, domains with interchanged a and b axis form, leading to a much smaller overall distortion of the sample. The domain formation seems also responsible for the observed transport anisotropy [6]. The lattice expansion perpendicular to the in-plane field is compatible with the proposed orbital ordering in $\text{Sr}_3\text{Ru}_2\text{O}_7$ [10–12]. In general, our observation represents a fascinating example of a structural relaxation driven by strong electronic correlations. Compared to the recently discussed nematic ordering in iron pnictides [5], the lattice distortion in $\text{Sr}_3\text{Ru}_2\text{O}_7$ occurs at 100 times lower temperatures and is more than 100 times smaller. Most remarkably it is not accompanied by magnetic ordering and represents the first example of a lattice instability in the immediate vicinity of a QCP.

We thank A. S. Gibbs, A. P. Mackenzie, R. Küchler, and M. Garst for collaborative work and S. A. Kivelson and C. Wu for helpful conversations. This work is supported by the German Science Foundation through SFB 602.

-
- [1] S. A. Kivelson, E. Fradkin, and V. J. Emery, *Nature (London)* **393**, 550 (1998).
 - [2] E. Fradkin *et al.*, *Annu. Rev. Condens. Matter Phys.* **1**, 153 (2010).
 - [3] M. P. Lilly *et al.*, *Phys. Rev. Lett.* **82**, 394 (1999).
 - [4] R. Daou *et al.*, *Nature (London)* **463**, 519 (2010).
 - [5] J.-H. Chu *et al.*, *Science* **329**, 824 (2010).
 - [6] R. A. Borzi *et al.*, *Science* **315**, 214 (2007).
 - [7] S. A. Grigera *et al.*, *Science* **294**, 329 (2001).
 - [8] S. A. Grigera *et al.*, *Science* **306**, 1154 (2004).
 - [9] J.-F. Mercure *et al.*, *Phys. Rev. B* **81**, 235103 (2010).
 - [10] S. Raghu *et al.*, *Phys. Rev. B* **79**, 214402 (2009).
 - [11] W.-C. Lee and C. Wu, *Phys. Rev. B* **80**, 104438 (2009).
 - [12] W.-C. Lee and C. Wu, arXiv:1008.2486.
 - [13] P. Gegenwart *et al.*, *Phys. Rev. Lett.* **96**, 136402 (2006).
 - [14] A. W. Rost *et al.*, *Science* **325**, 1360 (2009).
 - [15] Earlier magnetostriction measurements along the a axis at $\Theta = 0$ [16] have revealed a bifurcation of the transition at B_{c2} , which, however, has not been reproduced in the present experiments. Presumably it had been caused by stress during the cooldown of the sample.
 - [16] C. Stingl, R. S. Perry, Y. Maeno, and P. Gegenwart, *Phys. Status Solidi B* **247**, 574 (2010).
 - [17] S. A. Kivelson (private communication).
 - [18] J.-F. Mercure *et al.*, *Phys. Rev. Lett.* **103**, 176401 (2009).
 - [19] C. Wu (private communication).
 - [20] F. Weickert *et al.*, *Phys. Rev. B* **81**, 134438 (2010).